

Advances in the Rational Design of Rhodium Nanoparticle Catalysts: Control via Manipulation of the Nanoparticle Core and Stabilizer

Yuan Yuan, Ning Yan, and Paul J. Dyson*

Institut des Sciences et Ingénierie Chimiques, Ecole Polytechnique Fédérale de Lausanne (EPFL), CH-1015 Lausanne, Switzerland

ABSTRACT: This review describes some of the fascinating advances in the field of rhodium nanoparticle (NP) catalysis that have emerged in recent years. The examples described are categorized according to the research approach applied, involving either direct engineering of the NP core (size/shape control) or manipulating the NP via a stabilizer and/or solvent. Consequently, both surface-immobilized heterogeneous Rh NP and solvent dispersed Rh NP catalysts are included. The interplay between relevant parameters and the catalytic properties of Rh NPs are discussed, with a focus on design, function, and mechanisms. Rh NP-based multifunctional systems are also described. The approaches used to probe Rh NP catalysts at a molecular level and possible future research trends are highlighted.

KEYWORDS: rhodium, nanoparticle, heterogeneous catalysis, quasi-homogeneous catalysis, nanocatalysis



1. INTRODUCTION

Since the discovery of rhodium in 1803¹ there was little interest in the applications of the element until its critical role in catalysis was discovered.^{2–6} Indeed, rhodium exhibits extraordinary and often unique catalytic properties compared to most other metals, particularly in hydrogenation, carbonylation, hydroformylation, and oxidation reactions. About 80% of the worldwide annual production of rhodium (corresponding to 22 tons in 2009),⁷ is used in the fabrication of three-way catalytic converters in automobiles, catalyzing both reduction and oxidation reactions,⁸ and hence, rhodium is and will continue to be one of the rarest and the most costly metals. Although rhodium can be extracted from waste nuclear fuels this source is currently not cost-effective and the process has not been scaled-up.⁹ Combined, the preciousness of rhodium and its indispensability in catalysis drive research aimed at making the best use of this rare element.

Rhodium-based catalysts are generally classified into two main categories, supported heterogeneous catalysis and dispersed homogeneous catalysis, although many themes and variations exist. Solvent dispersed rhodium nanoparticles (NPs) represent an area where traditional homogeneous catalysis and heterogeneous catalysis converge. It has been known for many years that the size of rhodium particles immobilized on solid supports in heterogeneous catalysts are often of nanoscale dimensions, nevertheless, recent advances in nanoscience enable the precise characterization of NPs and open the way for a more rational control of their catalytic properties. In certain apparently homogeneous catalytic systems employing rhodium complexes it has been found that the actual catalytically active species are Rh NPs. For example, the RhCl₃–Aliquat 336 combination is widely used for the hydrogenation of various arenes including benzene,¹⁰ naph-

thalenes,¹¹ and other polyaromatic compounds.¹² The active catalyst was originally presumed to be composed of the solvated ion pair [(C₈H₁₇)₃NMe]⁺[RhCl₄]⁻,^{13,14} but a detailed mechanistic study demonstrated that the active catalyst corresponds to Rh NPs.¹⁵ Exceptional research on Rh NP catalysis has been reported in the past few years with efforts emanating from researchers from varied backgrounds. Most of these recent studies focus on two main strategies: (1) direct manipulation of the Rh NPs, an approach that is more common in heterogeneous catalysis and (2) the design of tailor-made stabilizers that indirectly modify the properties of the Rh NPs. Accordingly, this review is divided into two main parts, the first exploring how the size and shape of Rh NPs influence their catalytic properties, and the second being a critical analysis of the ways in which stabilizers and solvents can influence and even transform the catalytic properties of Rh NPs. The interplay between various parameters and the relevant catalytic properties of Rh NPs are discussed in both sections. In this review, emphasis is given to the most recent progress related to Rh NP catalysis, with the majority of cited references from 2006 onward. Earlier literature has been comprehensively discussed in a number of excellent reviews.^{16–19} Moreover, bimetallic^{20–26} and trimetallic²⁷ NP alloys containing rhodium and a detailed account of the effects of solid supports on heterogeneous rhodium catalysts²⁸ are also beyond the scope of this review.

Received: February 28, 2012

Revised: April 17, 2012

Published: April 18, 2012

2. ENGINEERING THE RH NP CORE

It is well-known that NP size has a profound influence on catalysis.^{29–33} The most apparent size-dependent feature being the increased percentage of surface atoms with decreased diameter, but this is not the only factor that determines the relationship between the diameter of Rh NP and its catalytic performance. Indeed, significantly different surface activities are often observed as the size of Rh NPs is varied.

Like the element itself, Rh NPs generally have a face-centered cubic structure and a hypothetical cuboctahedron represents a good model to describe their surface structure. There are four types of atoms on the surface, and depending on the coordination number, these atoms may be described by the symbols C₅ (corner atoms), C₇ (edge atoms), C₈ ((100) face atoms) and C₉ ((111) face atoms). These different atoms and the percentage of each type as a function of size are illustrated in Figure 1. It is evident that as the size of the NP increases, the

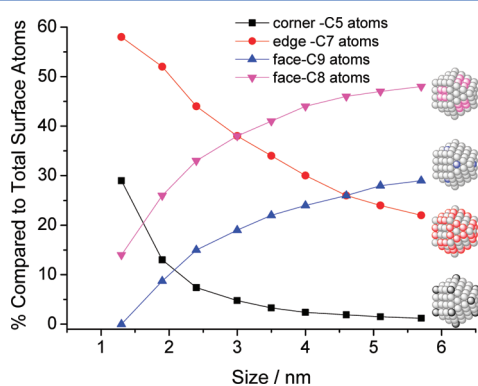


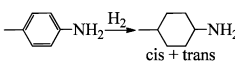
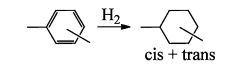
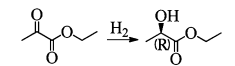
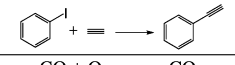
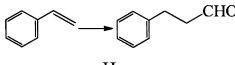
Figure 1. Percentages of different types of surface atoms as a function of particle size (based on a cuboctahedron model).

ratio between face atoms (C₈ and C₉) and total surface atoms (C_s) increases whereas the C₅:C_s and C₇:C_s ratios decrease. As a result, a positive size effect (also called a sympathetic size effect) is observed for reactions that have a tendency to occur at lower coordination sites such as C₅ and C₇ atoms, whereas a negative (antipathetic) size effect is observed for reactions that occur more rapidly on face atoms (C₈ and C₉).

Another factor that contributes to the size effect in Rh NP catalysis originates from size dependent chemical properties. Smaller Rh NPs generally contain a higher portion of electropositive Rh atoms on the surface. Moreover, the smaller the Rh NPs the more prone they are to oxidation. Therefore, a strong size effect appears if Rh_xO_y is the active catalytic species, catalytically inactive, or promotes side reactions, whether the reaction itself is conducted under an oxidative atmosphere or not. Table 1 collates studies on size effects of Rh NP catalysts. Analysis of the size dependent geometrical and chemical properties of the Rh NPs is complicated by the different supports/stabilizers; however, the majority of these data may be rationalized by considering these factors.

Initial investigations of CO oxidation on Rh single crystal surfaces³⁴ suggest that the reaction exhibits structure insensitive behavior at elevated pressures and temperatures, that is, the observed catalytic activity does not depend upon the underlying crystal structure.³⁵ However, Rh NP catalyzed CO oxidation can be size sensitive, as recently shown by Somorjai and co-workers. A series of polyvinylpyrrolidone (PVP) stabilized Rh NPs (2–11 nm) with narrow size distributions were synthesized and deposited on silicon wafers by Langmuir–Blodgett deposition.³⁶ A positive particle size effect was observed in the oxidation of CO. As the particle size decreases from 11 to 2 nm the turnover frequency (TOF) for the reaction at 200 °C increases 5-fold, and the apparent activation energy decreases from 28 to 19 kcal mol⁻¹. In situ synchrotron ambient pressure X-ray photoelectron spectroscopy (APXPS)

Table 1. Size Dependent Rh NP Catalyzed Processes

Size range(nm)	Stabilizer/support	Reaction	Size-activity relationship	Size-selectivity relationship	Ref.
5-30	γ -Al ₂ O ₃	$\text{CO} \xrightarrow{\text{H}_2} \text{C}_x\text{H}_y + \text{oxygenates}$	Negative size effect	Oxygenates increase as size decreases	52
1.2-3.5	SiO ₂		Negative size effect	Small NPs give a higher cis/trans ratio	40
2.3-7.8	MWNTs*		Negative size effect	Small NPs give a higher cis/trans ratio	41
0.96-1.65	Quinine/Al ₂ O ₃		Negative size effect	Large NPs give a higher ee	53
2-8	γ -Al ₂ O ₃		Negative size effect	-	54
2-11	PVP	$\text{CO} + \text{O}_2 \rightarrow \text{CO}_2$	Positive size effect	-	36
1.6-8	CeO ₂ , SiO ₂	$\text{CO} + \text{O}_2 \rightarrow \text{CO}_2$	Positive size effect	-	38
1-7	SiO ₂	$\text{C}_4\text{H}_{10} \xrightarrow{\text{H}_2} 2 \text{C}_2\text{H}_6$	Positive size effect	-	45
1-9	ZrO ₂	$\text{CH}_4 + \text{H}_2\text{O} \rightarrow \text{CO} + \text{H}_2$	Positive size effect	-	39
2.7-15	[C ₄ mim][BF ₄]	1-Hexene $\xrightarrow{\text{CO} + \text{H}_2}$ Heptanal (Linear + Branched)	Activity goes through a maximum at 5 nm	-	44
1-7	SiO ₂	$\text{C}_2\text{H}_4 \xrightarrow{\text{CO} + \text{H}_2}$ Propionaldehyde	Activity goes through a maximum at 2.5 nm	-	45
<1.5-6	SiO ₂		Activity goes through a maximum at 1.5-2 nm	-	55
0.7-6	ZrO ₂	$\text{C}_2\text{H}_4 \xrightarrow{\text{H}_2} 2 \text{CH}_4$	Activity goes through a maximum at 1.5 nm	-	50

* Multiwalled carbon nanotubes.

was used to monitor the oxidation state on the surface of the Rh NPs during the reaction. The most significant finding was the demonstration of the active catalyst being a surface oxide, the formation rate of which is inversely correlated to the NP size, that is, the amount of rhodium oxide species formed increases with decreasing NP size. This study was the first to show the active phase of a Rh NP catalyst during CO oxidation by XPS and providing insights into the size dependency of the reaction.

Further investigations of the size-dependent activity of these NPs were performed on high surface area mesoporous silica (SBA-15).³⁷ For uncalcined catalysts the particle size dependence observed in the CO oxidation reaction is similar to the trend observed in the study in which the Rh NPs were deposited on silicon wafers. If the catalyst is calcined (treated with O₂ at high temperature) and then reduced again in situ with H₂, a decrease in catalytic activity is observed and there is no longer a dependence on the particle size. IR spectroscopy was used to study CO adsorption on the uncalcined and calcined catalysts and revealed that CO adsorbed at bridging sites before calcination but on top sites after calcination. The change in adsorption geometry and oxidation activity may therefore be attributed to the interaction between PVP and the Rh surface. The uncalcined catalysts with intact PVP on the surface result in preferential adsorption of CO at bridging sites, which may cause an increase in catalytic activity and may be responsible for the positive size dependence observed in the oxidation of CO.

A size dependent effect was also observed for CO oxidation using ceria supported Rh NPs,³⁸ with the main observations agreeing with the previous findings, that is, smaller Rh NPs are more catalytically active. In situ X-ray absorption spectroscopy indicates that the high activity of the very small (1.3 nm) Rh NPs is related to a nearly complete oxidation of the Rh NPs under the reaction conditions, whereas NPs larger than 4 nm maintain their metallic state. In addition, the support also influences the oxidation behavior of the Rh NPs and therefore the catalytic activity. Compared to PVP-stabilized Rh NPs, where the size dependency disappears after calcination, the Rh NPs supported on ceria exhibit size dependent activity even after treatment at 450 °C. The same set of catalysts was also evaluated in methane steam reforming.³⁹ The intrinsic rate per surface Rh atom increases linearly with the Rh metal dispersion, that is, the catalytic activity decreases with increasing Rh particle size. The kinetic data imply that the overall reaction rate is controlled by the density of low-coordinated C₇ and C₅ atoms on the NPs. The step edge sites apparently provide a facile reaction pathway for C–H bond cleavage reactions and C–O recombination reactions compared to the C₈ and C₉ sites, and therefore a positive size effect is observed. However, Rh NPs smaller than 2.5 nm deactivate more rapidly than larger catalysts, because of the oxidation of the very small particles under the reaction conditions.

Silica supported Rh NP catalysts prepared by incipient-wetness were studied in the hydrogenation of *p*-toluidine.⁴⁰ Essentially, the pores on the silica are filled with aqueous RhCl₃, and then the silica is dried and reduced under a stream of H₂ and N₂ gases. A linear increase in TOF with increasing NP size, that is, a negative particle size effect, was observed in the hydrogenation reaction. As mentioned above, the increase in Rh NP size results in an increase of the face surface atoms (C₈ and C₉) and a decrease of the edge (C₇) and corner (C₅) sites, and therefore these results suggest that the hydrogenation

reaction takes place on the plane face surface (such as C₉ sites) as opposed to the C₇ and C₅ sites. This finding was corroborated in another study that investigated the hydrogenation of neat *o*-, *m*-, and *p*-xylene by Rh NPs immobilized on a carbon nanotube support.⁴¹ An increase in TOF of about 20% was observed as the size of the NPs increases from 2.3 to 4.5 nm, increasing by another 20% for NPs of 7.8 nm. The negative particle size effect again indicates that hydrogenation of the aromatic ring takes place on the C₉-centered sites. It is likely that the aromatic ring binds to more than one metal atom, for example, each double bond in the ring interacting with a metal in a trimetallic face, as this provides greater activation toward hydrogenation than binding to only one metal atom.⁴²

Negative particle size effects have also been observed in the transformation of CO into alkanes and oxygenates. Alumina-supported Rh NP catalysts of different sizes were prepared from microemulsions by varying the surfactant-to-oil ratio. The TOF increases about 4-fold as the Rh particle size increases from <5 to 30 nm. The higher TOF value provided by the larger Rh NPs appears to be mainly due to an increase in the CO dissociation rate. The selectivity was also found to be size dependent with smaller NPs favoring the formation of methane and oxygenated compounds. XPS revealed that the metal–support interaction increases with decreasing particle size, leading to the formation of partially oxidized Rh atoms that are responsible for oxygenate formation, explaining the increased selectivity for oxygenates over small Rh NPs. Density functional calculations were used to investigate C₁H_xO_y and C₂H_xO_y oxygenate formation routes on stepped (C₇ atoms) and flat (C₉ atoms) Rh surfaces. Energy profiles for the mechanistic pathways to oxygenates are lower on stepped surfaces, indicating a preference for low coordinated Rh sites, further rationalizing the higher selectivity for oxygenates by smaller NPs.⁴³

Ionic liquid (IL) dispersed Rh NPs with different sizes (2.7, 5.0, and 15 nm) have been evaluated in the hydroformylation of 1-hexene to heptanal.⁴⁴ A strong influence of the NP size on the hydroformylation reaction was observed with both the 2.7 and 15 nm NPs being less catalytically active than the NPs with a diameter of 5 nm. The chemoselectivity (the linear/branched ratio) is also lower with 2.7 and 15 nm NPs compared to the 5 nm Rh NPs. An induction period for the reaction suggests that leached Rh species from the NPs play a significant role in the observed catalytic activity and hinder a full rationalization of the size-activity relationship. The study was, however, corroborated by in situ spectroscopic investigations.⁴⁵

Five Rh/SiO₂ model catalysts with sizes ranging from 1.6 to 7.1 nm were evaluated in the hydroformylation of ethylene. The surface-specific activity was found to increase as the size of the Rh NPs decreases from 7.1 to 3.0 nm, reaching a maximum for the 2.5 nm Rh NPs (a ca. 4-fold higher activity compared to the 7.1 nm NPs), before decreasing significantly for the smallest (1.6 nm) Rh NPs. The first regime of reactivity (corresponding to the range 2.5–7.1 nm) demonstrates that propionaldehyde formation occurs more favorably on under-coordinated C₇ and C₅ Rh sites. Interestingly, the observed 4-fold activity increase in this regime is consistent with the increase in C₅ and C₇ Rh surface sites expected from this size decrease (see Figure 1), which increase in abundance by 5- and 2-fold, respectively. To explain the unusual second regime of reactivity (corresponding to a NP size of 1.6–2.5 nm), in situ IR spectroscopy was used to reveal the surface properties of different sized Rh NPs.

Under the solvent free conditions employed dispersed Rh carbonyl hydride Rh(CO)H species were observed on the surface of the smallest NPs, but not on the larger NPs, suggesting that the decreased activity of the 1.6 nm Rh NPs might be attributed to the formation of (unreactive) Rh(CO)H species. However, under typical industrial conditions of hydroformylation reactions, heterogeneous catalysts are often transformed into active homogeneous species containing both carbonyl and hydride ligands.^{46,47}

Hydrogenolysis of ethane to methane is a classical structure-sensitive reaction used initially by Sinfelt and co-workers to examine the effects of metal particle size on catalytic activity.^{48,49} An increase in surface catalytic activity with a decrease in particle size for supported platinum group catalysts is usually observed. However, a recent study suggests that such a positive size effect is only valid for Rh NPs larger than 1.5 nm.⁵⁰ ZrO₂-supported Rh particles with nanometer and subnanometer dimensions (0.7–6 nm) and very narrow particle size distributions were prepared using G4OH-PAMAM dendrimers as templates. As the Rh NP size decreases from 6 to 1.5 nm the catalytic activity was found to increase. However, a substantial decrease in TOF is observed as the particle diameter decreases below 1.5 nm. In keeping with investigations on Ru/SiO₂ catalyzed ethane hydrogenolysis⁵¹ it appears that an ensemble of at least 20 Rh atoms is required for the reaction to occur, and the surface Rh atoms on <1.5 nm particles do not reach this critical size.

As far as we are aware a negative size effect is always observed in the hydrogenation of aromatic substrates, where the absorption of the planar moiety on the surface atoms of Rh NPs is critical. The Fischer–Tropsch reaction also appears to display a negative size effect, but more mechanistic investigations are required to achieve a fuller understanding of the role of NPs in this reaction.

Spherical or near-spherical Rh NPs (cuboctahedrons), with both (100) and (111) facets exposed on the surface, are formed in uncontrolled synthesis.^{17,56} Shape controlled synthesis of Rh NPs enables the selective exposure of a certain facet, that is, (111) facets are exclusively exposed in tetrahedral Rh NPs whereas cubic Rh NPs are covered by (100) facets. Rh NPs with various morphologies including cubes,^{57–59} tetrahedra,⁶⁰ octahedra,⁶¹ multipods,⁶² icosahedra,⁶³ and triangular plates⁶³ have all been prepared. Despite these examples of shape-controlled synthesis, systematic studies that explicitly link catalytic performance to the shape of Rh NPs are limited.⁶³ In a very recent review on the shape dependent catalytic properties of metal NPs no examples based on rhodium were given.⁶⁴ Nevertheless, some very interesting and encouraging results have recently been obtained on the catalytic properties of tetrahedral Rh NPs.⁶⁰ Tetrahedral Rh NPs, obtained by thermal decomposition of [Rh(μ -Cl)(CO)₂]₂ in oleylamine at 170 °C and immobilized on charcoal, were compared with spherical Rh NPs (see Figure 2 for their transmission electron microscopy (TEM) images) in the hydrogenation of anthracene. Remarkably, the tetrahedral Rh NPs are 6-times more active than the spherical NPs and over 100-fold more active than commercial Rh/C. The selectivity (hydrogenation of the central ring vs side rings) of the tetrahedral Rh NPs is much higher than those of spherical NPs and commercial Rh/C. The superior catalytic performance of the tetrahedral NPs is presumably due to the faces of the tetrahedral nanocrystals comprising solely the more active (111) lattice planes, whereas

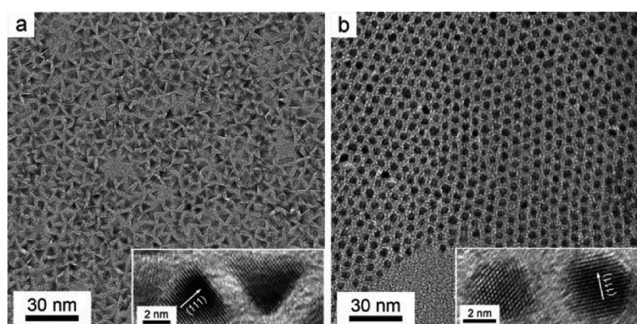


Figure 2. TEM and HR-TEM images (inset) of (a) tetrahedral (4.9 ± 0.4 nm) and (b) spherical (4.8 ± 0.4 nm) Rh NPs. Reprinted with permission from reference 60. Copyright 2007 John Wiley and Sons.

the spherical catalysts expose both (111) and less active (100) planes.

A comparative study of the catalytic activity of Rh nanopolyhedra and nanocubes in the reduction of nitric oxide by CO,⁶⁵ a reaction that takes place in a three-way catalytic converter, reveals that the TOFs were higher for the nanocubes compared to the nanopolyhedra. The activation energy for N₂ formation was lower on the Rh nanocubes than on Rh nanopolyhedra catalysts (22 versus 27 kcal mol⁻¹). The different catalytic performance of the two types of NPs may be rationalized by the surface planes exposed. It has been demonstrated previously for rhodium single crystals that Rh (100) single crystals are more active than the Rh (111) single crystals in NO reduction, probably because the reaction between CO and O is faster on the (100) surface than on the (111) surface. The NO dissociation product also has a higher heat of adsorption on the (100) facet.⁶⁶ The higher activity of the Rh nanocubes therefore correlates with the higher expose of the more active (100) planes.

Rh NPs with different morphologies can be prepared in aqueous solution in the presence of sodium lauryl sulfate (SLS) and NaX (X = F, Cl, Br) salts.⁶⁷ Horn-, cube-, and dendritic-shaped particles were obtained in the presence of NaCl, NaBr, and NaF, respectively (see Figure 3 for TEM images). The shape-dependent catalytic properties of these Rh particles were assessed in the electro-oxidation of ethanol. Current densities of 0.018, 0.022, and 0.035 mA cm⁻² were recorded for the cube-, horn-, and dendritic-shaped NPs, respectively, indicative of enhanced catalytic activity in the order: cube < horn << dendrites. A high electrochemically active surface area could be the key for the superior performance of the Rh nanodendrimers, but other factors may contribute as well, the most evident one being that the different halides, which were used in the synthesis of these Rh NPs and remain on the NP surface, are likely to be noninnocent in electro-catalytic reactions.

The shape of the Rh NPs can also change during catalysis, particularly under an oxidative atmosphere. Oxygen-induced shape transformations of Rh NPs on MgO (001) surfaces have been reported.⁶⁸ An in situ high-resolution X-ray diffraction (XRD) study revealed a reversible facet rearrangement of the Rh NPs on magnesia that was attributed to the formation of oxygen-induced superstructures.

3. NP MANIPULATION VIA THE STABILIZER

Most Rh NPs are synthesized in solution and are then used either directly or following immobilization on solid supports.

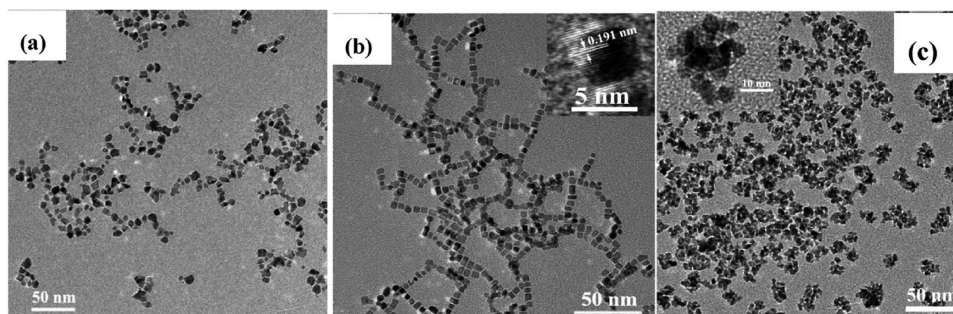


Figure 3. TEM images of Rh NPs with different morphologies: (a) horned particles prepared in H₂O with NaCl and SLS as the capping agents; (b) nanocubes prepared in H₂O with NaBr and SLS as the capping agents; and (c) nanodendrites prepared in H₂O with NaF and SLS as the capping agents. SLS = sodium lauryl sulfate. Reprinted with permission from reference 67. Copyright 2010 American Chemistry Society.

Although the general trend is to transform a successful solvent-dispersed NP catalyst into a heterogeneous one (see section 3.4),⁶⁹ there are many good reasons to use Rh NP catalysts dispersed in solvents. Freely dispersed Rh NPs possess higher surface areas and avoid internal mass transfer limitations; consequently the catalytic activity of Rh NPs in the solution phase may be higher than those anchored on solid supports. Furthermore, the functions of dispersed Rh NPs may be manipulated by tailoring the stabilizer, in addition to the more conventional approach involving size and shape control. Table 2 summarizes the reactions catalyzed by dispersed Rh NPs. Despite the advantages noted above solvent-dispersed Rh NPs are not without problems. Their solubility in desired solvents, stability under harsh conditions, and recyclability challenge their practical use. However, carefully designed stabilizers can help to overcome these limitations and may also endow Rh NPs with enhanced activities and exceptional selectivities.

Rh NPs tend to be soluble in a limited number of solvents which is an obstacle for their application as dispersed catalysts. PVP is perhaps the most widely used Rh NP stabilizer in catalytic applications, but its use is largely restricted to water and alcohols. To address this problem a family of PVP derivatives with adjustable polarity, that is, by varying the length of an alkyl chain attached to PVP, expands the range of solvents that can be used.⁹¹ The stabilizers, C₂-PVP (ethyl modified), C₄-PVP (butyl modified), C₆-PVP (hexyl modified), and C₈-PVP (octyl modified), afford Rh NPs that may be dispersed in a wide range of solvents (13 common solvents were tested ranging from polar to nonpolar), and as expected, as the length of the alkyl chain increases the hydrophobicity of C_n-PVP increases and solubility in less polar solvents improves (C₆-PVP-protected Rh NPs even disperse well in hexane).

In addition to increasing the range of accessible organic solvents for NP catalysis, ionic liquids (ILs) are also attractive solvents, facilitating liquid–liquid biphasic processes. Rh NPs stabilized by PVP tend to disperse poorly in common ILs, but simple functionalization of the IL overcomes this limitation. PVP is highly soluble in alcohols and water, and similarly, in ILs functionalized with a hydroxyl substituent.⁸¹ In comparison to PVP-stabilized Rh NPs in [C₂mim][BF₄] (where C₂mim = the 1-ethyl-3-methylimidazolium cation), in the hydroxyl-functionalized IL [C₂OHmim][BF₄] (where C₂OHmim = the 1-(2-hydroxyethyl)-3-methylimidazolium cation) they exhibit superior solubility (Figure 4). Because of the superior dispersion of the PVP-protected Rh NPs in [C₂OHmim][BF₄] considerably higher activities and stabilities are observed, as well as an excellent recycling and reuse.

Phase transfer agents may also be used to facilitate the dispersion of Rh NPs in different solvents. For example, water dispersed Rh NPs, stabilized with [HEA12]Cl (where HEA12 = the *N,N*-dimethyl-*N*-dodecyl-*N*-(2-hydroxyethyl)ammonium cation), undergo complete transfer into an IL phase comprising [HEA12][Tf₂N] (where Tf₂N⁻ is the (trifluoromethanesulfonyl)amide anion), upon addition of LiTf₂N. The resulting [HEA12][Tf₂N] stabilized Rh NPs may then be dispersed in [C₄mim][PF₆] (where C₄mim = the 1-butyl-3-methylimidazolium cation) and this latter system was shown to efficiently catalyze the hydrogenation of styrene to ethyl benzene.⁷⁴

NP stabilizers must offer more than ideal solubility properties with respect to their application in catalysis. The stability imparted on the NPs is also critical and yet, at the same time, high catalytic activity must also be possible. These two properties tend to be mutually exclusive with the most stable NPs being the least active and vice versa. Nevertheless, a number of Rh NPs coated by tailor-made stabilizers exhibit remarkable catalytic properties.

There are four main interactions involved in the stabilization of NPs, that is, electrostatic, steric, electrosteric, and coordination.¹⁶ Manipulation of the four interactions allows both catalyst stability and catalytic activity to be modulated in a synergistic fashion. For example, a copolymer derived from the PVP monomer unit and 1-vinyl-3-butylimidazolium chloride (poly(NVP-*co*-VBIM⁺Cl⁻), see Figure 5) provides Rh NPs with steric, coordinative, and electrostatic stabilization.⁷⁵ The copolymer was synthesized through the free radical polymerization of *N*-vinyl-2-pyrrolidone, and Rh NPs with a narrow unimodal size distribution of around 3 nm were obtained in [C₄mim][BF₄]. These NPs were found to show high activity and stability in the hydrogenation of benzene leading to unprecedented lifetimes (total turnovers >20,000) for this reaction. These Rh NPs were also used to hydrogenate a range of aromatic substrates with the partial reduction of certain substrates observed.⁷⁷

Derivatization of PVP with a carboxylate group provides a water and IL soluble polymer (PVP-CO₂Na) that potentially increases NP stability via the additional weak coordination of the carboxylate group with the metal surface, and via electrostatic stabilization, with the formation of a protective electronic double layer.⁸⁵ Rh NPs protected by the polymer PVP-CO₂N prepared in water have a narrow size distribution, with an average diameter of 4 nm, and exhibit superior thermal and catalytic stability than PVP coated NPs. In the hydrogenation of toluene, even at low stabilizer/Rh ratios (2:1), the Rh NPs can be reused multiple times without any loss of

Table 2. Examples of Reactions Catalyzed by Dispersed Rh NPs

Solvent	Stabilizer	Size (nm)	Precursor	Reaction	Conv.%	Sel.%*	TOF (h ⁻¹)	Ref.
water	THEA16Cl	2.5-3.5	RhCl ₃		100	78	120	70
water	HEA16BF ₄	2-6	RhCl ₃		100	100	3600	71
water	HEA16HCO ₃	2.5-3.5	RhCl ₃		100	100	2571	71
water	P[C ₆ H ₄ -p-(OCH ₂ CH ₂) _n OH] ₃	1.8±0.4	RhCl ₃		100	-	3333	72
water	PVP/ DiCyp-MPPMS	3.4±0.5	RhCl ₃		66	92	15	73
[C ₄ mim][PF ₆]	[HEA12][Tf ₂ N]	2.8	RhCl ₃		100	-	100	74
[C ₄ mim][BF ₄]	poly(NVP-co-VBIM ⁺ Cl)	2.9±0.6	RhCl ₃		100	100	250	75
[C ₄ mim][BF ₄]	[C ₄ mim][BF ₄]	4	RhCl ₃		100	-	1000	76
[C ₄ mim][BF ₄]	poly(NVP-co-VBIM ⁺ Cl)	3.0±0.8	RhCl ₃		37	62	62	77
[C ₄ mim][PF ₆]	TPTZ	3.5-4.5	RhCl ₃		100	96	7	78
[C ₄ mim][PF ₆]	TPPZ	-	RhCl ₃		100	30	7	78
[C ₄ mim][PF ₆]	2,2'-Bipy	2	RhCl ₃		100	60	7	78
[C ₄ mim][PF ₆]	3,3'-Bipy	2.0-2.5	RhCl ₃		100	100	7	79
[C ₄ mim][PF ₆]		-	RhCl ₃		85	-	17	80
[C ₄ mim][PF ₆]	4,4'-Bipy	2.0-2.5	RhCl ₃		100	100	7	79
[C ₂ OHmim][BF ₄]	PVP	2.7	RhCl ₃		100	99.8	2000	81
[C ₄ mim][BF ₄]	-	1.7±0.3	Rh ₆ (CO) ₁₆		90	-	695	82
[C ₄ mim][Tf ₂ N]	-	2-3	RhCl ₃		98	84	74	83
[C ₄ mim][Tf ₂ N]	[BIHB][Tf ₂ N] ₂	1-2	RhCl ₃		ca. 96	100	16	84
[C ₂ OHmim][BF ₄]	[CO ₂ Na-PVP][C ₈ mim]	-	RhCl ₃		97	100	243	85
[Bu ₄ N]Br	-	3.3±1.5	Rh(acac)(CO) ₂		-	-	8800	86
N(C ₆ H ₁₃) ₄ Br	-	2.8 ± 0.7	Rh(acac) ₃		40	42	39	87
[C ₄ mim][PF ₆]	-	5-10	Rh(OAc) ₃		98	44	13	87
[C ₄ mim][PF ₆]	-	-	RhCl ₃		84	47	7	88
	[PPh ₂ dmim][Tf ₂ N]	2.4 ± 0.6	Rh(allyl) ₃		100	-	33	89
Methanol	PAMAM G4-OH	1.8±0.4	RhCl ₃		-	-	22	90
Ethanol	C ₄ -PVP	3.2±0.5	RhCl ₃		-	-	566	91
1-pentanol/water	Ph ₂ P(CH ₂ CH ₂ O) ₂₂ CH ₃	2.2±0.2	RhCl ₃		99	100	1000	92
Toluene	Dimethylammonium Hexanoate	2.3 ± 0.8	[(C ₅ H ₁₁ CO ₂) ₂ Rh]	2NHMe ₂ BH ₃ → [NMe ₂ BH ₂] ₂ + 2H ₂	100	-	630	93

*For reactions that produce more than one product the selectivity corresponds to the first product shown.

activity whereas PVP stabilized Rh NPs deactivate rapidly when applied under the same conditions. TEM images of the Rh NPs before and after catalysis show that those coated with PVP-

CO₂Na are significantly resistant to agglomeration unlike those protected by PVP (see Figure 6). IR spectroscopy and XPS analysis both indicate that the carboxylic acid group and amide

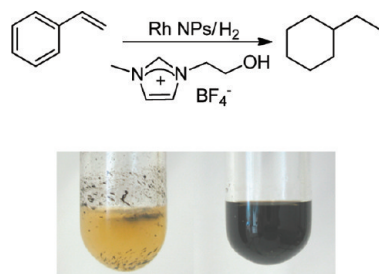


Figure 4. PVP-protected Rh NP catalyzed styrene hydrogenation (top) and photographs of the Rh NPs dispersed in $[\text{C}_2\text{mim}][\text{BF}_4]$ (bottom left) and the hydroxyl-functionalized IL $[\text{C}_2\text{OHmim}][\text{BF}_4]$ (bottom right).

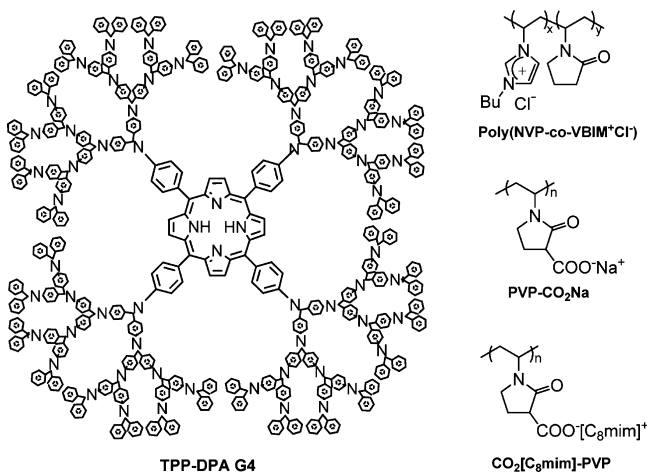


Figure 5. Examples of polymers used to modulate the catalytic performance of Rh NPs.

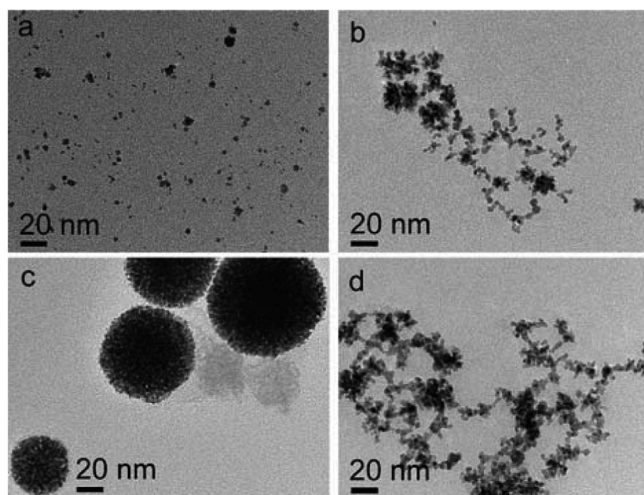


Figure 6. TEM images of Rh NPs stabilized by (a) PVP; (b) PVP- CO_2Na ; (c) PVP after 5 catalytic batches; (d) PVP- CO_2Na after 5 catalytic batches.⁸⁵ Reproduced with permission from reference 85. Copyright 2011 Royal Society of Chemistry.

functionality in the polymer interact with the Rh NP surface. Exchange of the Na^+ ion by $[\text{C}_8\text{mim}]^+$ (where C_8mim = the 1-octyl-3-methylimidazolium cation) provides IL soluble Rh NPs that can also be used in biphasic catalysis.

Rh NPs have been encapsulated within a fourth generation phenylazomethine dendrimer (TPP-DPA G4, see Figure 5) and a polyamidoamine dendrimer (PAMAM G4-OH).⁹⁰ The

synthetic strategy involves impregnation and coordination of 60 equiv of RhCl_3 within the dendrimer followed by reduction to form the Rh NPs. A MALDI-TOF mass spectrum of the TPP-DPA G4 system contained a peak at about 17 KDa indicating that approximately 58 rhodium atoms are encapsulated in a single dendrimer molecule, which is close in value to the expected stoichiometry. Catalytic evaluation of these Rh NP-dendrimer systems in the hydrogenation of olefins and nitroarenes afforded high TOFs (up to 17520 h^{-1}) indicating that substrates are not hindered by the branches of the dendrimers. Immobilization of the dendrimers on solid supports, for example, ZrO_2 , provided a reusable, heterogeneous catalytic system.⁵⁰

In addition to macromolecular polymer and dendrimer NP stabilizers, small molecule “ligands” are attractive stabilizers as their steric and electronic properties can be carefully designed and modified to provide a molecular-level understanding of the role of the stabilizer with respect to catalytic function. Rh NPs coated with various bipyridine ligands (2,2′-, 3,3′-, and 4,4′-bipy, see Figure 7) dispersed in $[\text{C}_4\text{mim}][\text{PF}_6]$ were found to effectively catalyze the hydrogenation of arenes.^{79,94} The activity in terms of the complete reduction of styrene to ethylcyclohexane follows the order $3,3′\text{-bipy} \approx 4,4′\text{-bipy} > 2,2′\text{-bipy}$. It is conceivable that 2,2′-bipy coordinates to the Rh NP surface via both N-donor atoms (see Figure 8) whereas 3,3′-bipy and 4,4′-bipy coordinate to the Rh NPs via only one N atom; thus 2,2′-bipy would bind more strongly than the other two ligands leading to the lower catalytic activity (ligand dissociation is required to generate the active catalyst). This hypothesis was validated by the selective alkylation of one of the N-donor atoms in 2,2′-bipy rendering it a monodentate ligand, and in subsequent catalytic tests it was found to give a more active catalyst. Bipyridine ligand stabilized Rh NPs also catalyze the hydrogenation of lignin model compounds such as anisole and cresols.⁹⁵ Various poly-N-donor ligands (e.g., TPPZ and TPTZ shown in Figure 7) were also studied and shown to give comparable catalytic activities.⁷⁸

Both mono- and bis-imidazolium functionalized 2,2′-bipyridine ligands (see Figure 7) have been explored as Rh NP catalyst stabilizers in catalytic applications in ILs.^{80,84} The two bis-imidazolium functionalized bipyridines, $[\text{BIMB}][\text{Tf}_2\text{N}]_2$ and $[\text{BIHB}][\text{Tf}_2\text{N}]_2$ are both sterically and electronically distinct, the latter being sterically less demanding because of the greater distance of the imidazolium group from the bipyridine moiety. $[\text{BIHB}][\text{Tf}_2\text{N}]_2$ is a stronger ligand than $[\text{BIMB}][\text{Tf}_2\text{N}]_2$ as the electron withdrawing effect of the imidazolium moiety is diluted by the C_7 alkyl chain (the electronics of the ligands were evaluated by spectroscopy). In the reduction of toluene the Rh NPs stabilized by $[\text{BIHB}][\text{Tf}_2\text{N}]_2$ were significantly more active and stable than those stabilized $[\text{BIMB}][\text{Tf}_2\text{N}]_2$ and 2,2′-bipy, which was attributed mostly to steric effects as $[\text{BIHB}][\text{Tf}_2\text{N}]_2$ is electronically similar to bipy.

Rh NPs stabilized by tetraalkylammonium salts in water exhibit spherical or so-called worm-like morphologies depending on the nature of the counteranion.⁷¹ With less nucleophilic anions which form only weak interactions with the NP surface, worm-like particles are formed which are poor catalysts in hydrogenation reactions, presumably because of having less active facets.

Ligands have also been used to modify the chemoselectivity of PVP-stabilized Rh NP catalysts in the hydrogenation of phenylacetone (Figure 9). Sulfonated, water-soluble phosphine

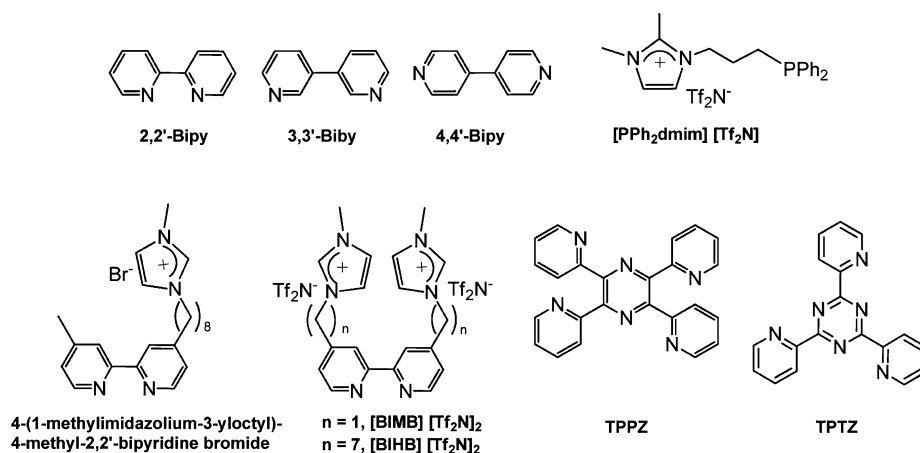


Figure 7. Examples of ligands used to modulate the catalytic performance of Rh NPs.

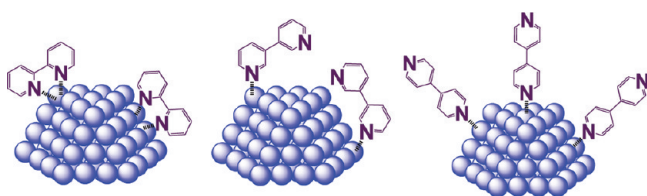


Figure 8. Representation of the possible coordination modes of 2,2'-bipy, 3,3'-bipy, and 4,4'-bipy on the surface of a Rh NP.

ligands with different steric and electronic properties were added to PVP-stabilized Rh NPs dispersed in water and shown to interact in different ways with the NP surface by IR spectroscopy using CO as a probe. The different ligands create unique microenvironments on the NP surface that influence chemoselectivity, presumably by preventing binding of the substrates to certain sites on the NP surface. Remarkably, in the presence of DiCp-MPPMS (Figure 9) hydrogenation of the C=O bond can be suppressed without significantly interfering with the hydrogenation of the aromatic ring allowing cyclohexylacetone to be obtained in high yield. Such high selectivity over Rh NPs is unprecedented although related reactions have been catalyzed by Ir NPs.⁹⁶

Chiral ligands, polymers, and surfactants have been used to modify the surface of pre-prepared Rh NPs affording, in most cases, enantioselective catalysts (see Figure 10 and Table 3). In addition to these examples, chiral dendrimers were also used to

protect Rh NPs, but their application in catalysis was not reported.⁹⁷

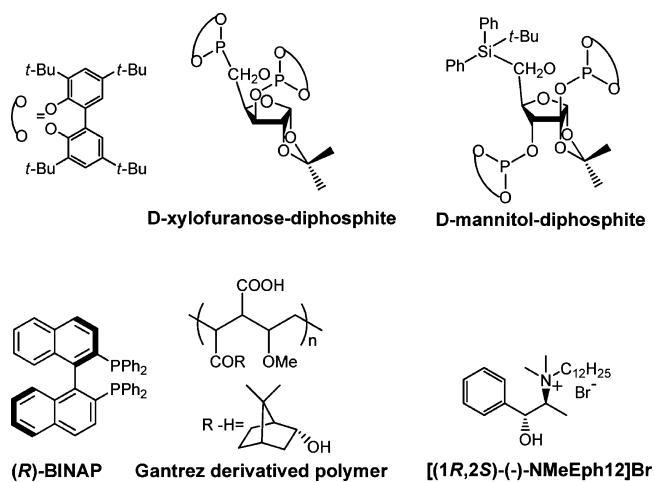


Figure 10. Chiral compounds used to modify the surface of Rh NPs for enantioselective catalysis.

Chiral mono- and diphosphine/phosphite modified Rh NPs supported on silica have been evaluated as catalysts in asymmetric hydroformylation reactions.⁵⁵ Enantioselectivities of up to 72% were obtained using (R)-BINAP as the modifier. The Rh NPs modified with chiral monophosphines gave much lower enantioselectivities, attributed to their inability to form a

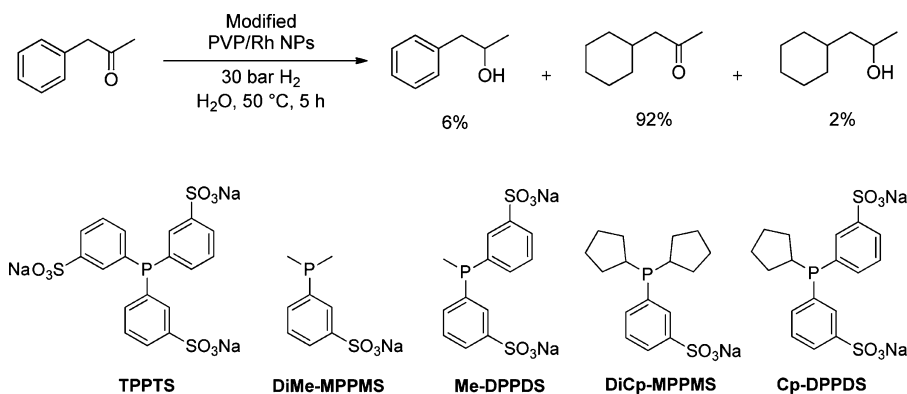


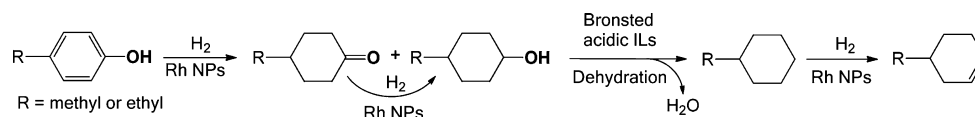
Figure 9. Chemoselective hydrogenation of phenylacetone by PVP-stabilized Rh NPs in the presence of water-soluble phosphine ligands.

Table 3. Examples of Enantioselective Reactions Catalyzed by Rh NPs^a

Ligands	Size (nm)	Precursor	Reaction	TOF (h ⁻¹)	ee (%)	b:n	Ref.
(<i>R</i>)-BINAP	1.5–2.0	RhCl ₃		11	72 <i>S</i>	100	55
(<i>R</i>)-BINAP	1.5–2.0	RhCl ₃		13	30 <i>S</i>	92:8	55
(<i>R</i>)-BINAP	1.5–2.0	RhCl ₃		22	26 <i>S</i>	89:11	104
D-xylofuranose-diphosphite	50	[Rh(μ-OMe)(cod)] ₂		92	40 <i>S</i>	>99	100
D-mannitol-diphosphite	35	[Rh(μ-OMe)(cod)] ₂		667	24 <i>S</i>	90	100
D-xylofuranose-diphosphite	1.6–4	Rh(η ³ -C ₃ H ₅) ₃		5–57	≤6	-	101
Gantrez derived polymer	3.5	RhCl ₃		40	0	-	102
(1 <i>R</i> ,2 <i>S</i>)-(-)-NMeEph12Br	2.5	RhCl ₃		100	12 <i>R</i>	-	103

^aNote that the Rh NPs may be precatalysts.

Scheme 1. Key Steps Involved in the Formation of Alkanes from Lignin Derived Phenols Catalyzed by Rh NPs Dispersed in Brønsted Acidic ILs



stable and rigid chiral environment on a metal surface partly because of the competitive absorption of CO. However, contributions from homogeneous complexes formed in situ by leaching of surface Rh atoms and reaction with the chiral ligands cannot be ruled out—in general complexes with chiral monodentate ligands display lower enantioselectivities than complexes with chelating chiral ligands.^{98,99}

NPs modified by chiral ligands in the absence of other stabilizers have also been studied with, for example, Rh NPs (2–3 nm) coated with D-xylofuranose-diphosphite or D-mannitol-diphosphite evaluated in the hydroformylation of styrene.¹⁰⁰ Remarkably, the NPs exhibit a slightly higher enantioselectivity than Rh complexes with the same ligand, although the activity is reduced. Mercury and CS₂ poisoning experiments do not significantly reduce the activity or selectivity, indicative of homogeneous catalysis, and furthermore, in situ HP NMR spectroscopic studies under hydroformylation conditions revealed the formation of molecular species. From these experiments it was concluded that the Rh NPs served as a reservoir for active molecular catalytic species indicating that the active catalyst generated in situ is different to the prepared complex. The same NPs were also used in the hydrogenation of *o*-methylanisole with a very low enantioselectivity (≤6%) observed.¹⁰¹

Rh NPs stabilized by polymers functionalized with chiral appendages (a Gantrez derived polymer, see Figure 10) were assessed as catalysts in the enantioselective hydrogenation of ethyl pyruvate, but no enantioselectivity was detected, even in the presence of cinchonidine (2 equiv).¹⁰² In contrast, the application of a chiral surfactant [(1*R*,2*S*)-(-)-NMeEph12]Br in place of the polymer results in low enantioselectivities of up to 12% in the asymmetric hydrogenation of ethyl pyruvate in water. Addition of the chiral inducer, (-)-cinchonine, further increases the enantiomeric excess (*ee*) to 18%.¹⁰³ However, these findings further point toward the formation of

homogeneous mononuclear species as the active catalyst in the presence of ligands, as the polymer is unable to form discrete complexes, and while the surfactant may act as a ligand it is a much less efficient ligand than the P-based ligands mentioned above.

Rh NPs catalyze a range of reactions including hydrogenation, dehydrogenation, and hydrogenolysis, and tandem reactions such as dehydrocoupling-hydrogenation reactions¹⁰⁵ and dehalogenation-hydrogenation reactions.^{106,107} The scope of tandem reactions can be broadened by immobilization of the Rh NPs in/on functional supports. For example, Rh NPs dispersed in Brønsted acidic ILs catalyze the upgrading of phenolic compounds, which are significant components in bio-oil.⁸³ The key steps in the formation of cyclohexanes from phenols, as an example, include catalyzed hydrogenations by the NPs combined with dehydration steps catalyzed by the Brønsted acid (see Scheme 1). An optimized bifunctional system was used to transform a variety of phenolic compounds with a conversion of 98% and a selectivity to cyclohexane of 84%. Compared to previous systems that are either performed with metal sulfite or with mineral acid/supported metal catalysts in water this NP system for upgrading lignin derivatives is much less energy demanding.

4. SEPARATION AND RECYCLING

Facile separation and recyclability are also required to achieve industrial implementation of dispersed metal NP catalysts.¹⁰⁸ The main approaches used to overcome separation (and hence contamination) problems include transfer of the Rh NPs onto a solid support to afford heterogeneous catalysts, the application of biphasic conditions in which the Rh NPs and the products efficiently separate, and the design of “smart” NPs that can be precipitated (and subsequently redispersed) via the application of external stimuli. The first approach is currently the method of choice despite often resulting in a decrease in activity after

immobilization.^{69,109} Although used for many years, recent trends involve the use of novel inorganic nanomaterial supports, such as graphene,^{110,111} carbon nanotubes,^{41,112–115} carbon nanofibers,^{116,117} porous carbon,¹¹⁸ porous ionic copolymer,¹¹⁹ nanocrystalline hydroxyapatite,¹²⁰ mesoporous aluminosilicates,¹²¹ aluminum oxyhydroxide nanofibers,¹²² cellulose-IL hybrid membranes,¹²³ nanosized SiO₂,¹²⁴ and mesoporous silica.¹²⁵ New ways to immobilize Rh NPs on solid supports have also been developed, for example, a dry impregnation method that involves spraying an aqueous solution of Rh NPs on porous silica particles, which avoids calcination and activation steps that may contribute to a reduced activity of the NPs.¹²⁶ A similar approach has also been applied to the preparation of highly active Rh/TiO₂ catalysts.^{106,127} A number of biphasic processes involving homogeneous catalysts are now used on an industrial scale,^{128–131} which should encourage the development of processes with NP catalysts. Indeed, immobilization of Rh NPs in solvents such as water, supercritical fluids, and ILs are now commonplace.^{82,132–134} Further details of these approaches for recycling NP catalysts, including Rh NP systems, may be found elsewhere.^{135–137}

The third strategy identified above, that is, involving stimuli-sensitive materials, although less well developed, could find certain niches. A magnetically recoverable Rh NP catalyst with extraordinary recycling properties has been reported.¹³⁸ The catalyst comprises about 60 nm silica spheres containing magnetic Fe₃O₄ cores (10 nm) functionalized on the surface with 3–5 nm Rh NPs (see Figure 11). The system is highly

catalytically active for the hydrogenation of cyclohexene and benzene, and could be reused up to 20 times (total turnovers: 180,000 for cyclohexene and 11,550 for benzene), with facile recovery by extraction with a magnet.

Alkyl modified PVPs exhibit thermomorphic properties—being soluble in water at low temperatures and precipitating once the temperature of the system increases above a critical point (the so-called lower critical solution temperature, LCST).¹³⁹ Carboxylate modified PVP is pH sensitive and is soluble in aqueous solutions at pH > 2.¹⁴⁰ These properties, combined with the ability to stabilize the NPs, enables recycling of a variety of metal NPs, including Rh NPs, via temperature or pH control.

5. CONCLUSIONS AND PERSPECTIVES

Considerable progress has been made in the development of highly efficient Rh NP catalysts, achieved by either engineering the Rh NP core or by stabilizer modification, with detailed mechanistic studies facilitating rational design. Direct manipulation of the Rh NPs may be divided into size and shape controlled approaches. Size dependent catalytic properties are comparatively well understood with positive, negative, and complicated size effects all possible depending on the reaction under study. Further comprehensive investigations devoted to understanding shape effects of Rh NPs in catalysis are needed. From the few examples reported, shape effects may be attributed to the different facets exposed by Rh NPs with different topologies. Whether other factors play a role in catalytic performance, with respect to NP shape, remains to be seen. NP stabilizers have proven to be far more than capping agents or templates in NP synthesis. Their ability to enhance the performance of Rh NP catalysts appears to have been underestimated until recently. Recent reports have unequivocally demonstrated that tailor-made stabilizers can be used to improve the activity, selectivity, stability, solubility, and recyclability of dispersed Rh NPs. As far as we are aware, a strategy that combines the two approaches, that is, a synthetic strategy that optimizes both the Rh NP core and the stabilizer, has yet to be realized. Moreover, very few examples of multifunctional catalytic systems involving Rh NPs have been reported to date.

Various mechanistic details will certainly facilitate the design of new Rh NP catalysts. For example, neither the chemical nor the geometrical factors of Rh NPs change dramatically as the NP size increases beyond 6 nm. This observation is in accordance with the fact that the most significant Rh NP size-effects were observed below 6 nm, and provides a guideline on the size range (1–6 nm) that should be focused on in Rh NP design. However, more detailed characterization studies and mechanistic studies are essential, especially for solvent dispersed Rh NP catalysts, which are less well characterized than their heterogeneous counterparts. Liquid supports appear to be extremely attractive, because of various properties described in this review, and may even be unwittingly used on an industrial scale—even Wilkinson's catalyst may decompose to form NPs under aggressive reaction conditions. It has been shown that certain Rh NPs are actually precursors to homogeneous catalysts.^{46,47} Therefore it may be safer to refer to Rh NP precatalysts and not catalysts. However, more extensive in situ mechanistic studies are required before generalizations of this type can be made, and in comparison to the field of palladium catalyzed coupling reactions, it took many years until a clear picture of the mechanism emerged. In

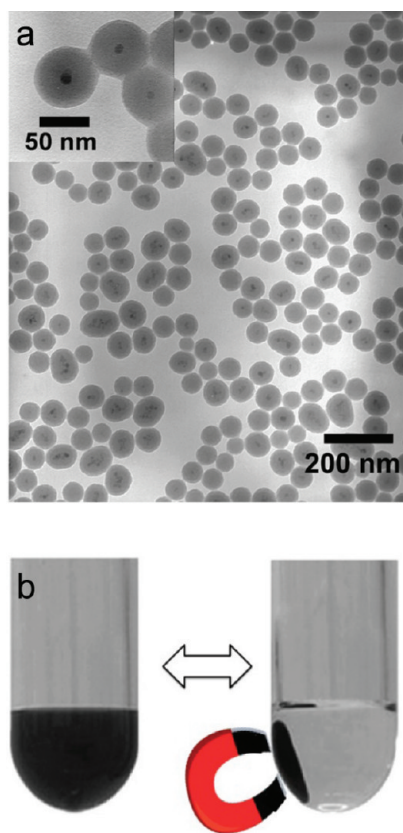


Figure 11. (a) TEM image of silica-coated magnetic particles and (b) illustration of the magnetic separation technique used. Reprinted with permission from reference 138. Copyright 2008 Elsevier.

this respect, it should be stressed that knowing whether the true catalyst is the NP, a mononuclear metal species, or potentially a small subnanometer cluster, is merely the first step in elucidating the mechanism which proved so vital in the palladium-coupling arena. To delineate full mechanistic details close collaborations between those studying heterogeneous catalysis and those focused on homogeneous catalysis might prove beneficial.

Another important trend in other areas of catalysis has been to replace expensive and rare metals with earth abundant and cheap metals. In this respect Co NPs must be worth studying further, especially when one considers that the majority of rhodium obtained today is used in automotive catalytic converters. With increasingly stringent environmental legislation and a rapid rise in car ownership a cheap alternative to rhodium would be welcome. Indeed, a Pt-Co/ γ -Al₂O₃ catalyst was recently tailored to mimic the microstructure of Pt-Rh NPs. The activity and selectivity of the new catalyst in the reduction of NO with H₂ is superior to that of Pt alone.¹⁴¹ The discovery of such catalysts is highly desirable for sustainable development that necessitates the use of earth abundant metals.

AUTHOR INFORMATION

Corresponding Author

*E-mail: paul.dyson@epfl.ch.

Funding

We thank the Swiss National Science Foundation and EPFL for financial support. N.Y. thanks the EU for a Marie-Curie Fellowship (No. 252125-TCPBRCBDP).

Notes

The authors declare no competing financial interest.

REFERENCES

- (1) Wollaston, W. H. *Philos. Trans. R. Soc. London* **1804**, *94*, 419–430.
- (2) Kaspar, J.; Fornasiero, P.; Graziani, M. *Catal. Today* **1999**, *50*, 285–298.
- (3) Kaspar, J.; Fornasiero, P.; Hickey, N. *Catal. Today* **2003**, *77*, 419–449.
- (4) Matsumoto, S. i. *Catal. Today* **2004**, *90*, 183–190.
- (5) Rossen, K. *Angew. Chem., Int. Ed.* **2001**, *40*, 4611–4613.
- (6) Ungvary, F. *Coord. Chem. Rev.* **2002**, *228*, 61–82.
- (7) Loferski, P. J., Ed.; *2009 Minerals Yearbook: Platinum-Group Metals*; U.S. Department of the Interior, U.S. Geological Survey: Washington, DC, 2011.
- (8) *Catalytic Air Pollution Control: Commercial Technology*; Heck, R., Farrauto, R., Eds.; Van Nostrand Reinhold: New York, 1995.
- (9) Kolarik, Z.; Renard, E. V. *Platinum Met. Rev.* **2005**, *49*, 79–90.
- (10) Blum, J.; Amer, I.; Zoran, A.; Sasson, Y. *Tetrahedron Lett.* **1983**, *24*, 4139–4142.
- (11) Amer, I.; Amer, H.; Blum, J. *J. Mol. Catal.* **1986**, *34*, 221–228.
- (12) Amer, I.; Amer, H.; Ascher, R.; Blum, J.; Sasson, Y.; Vollhardt, K. P. C. *J. Mol. Catal.* **1987**, *39*, 185–194.
- (13) Sasson, Y.; Zoran, A.; Blum, J. *J. Mol. Catal.* **1981**, *11*, 293–300.
- (14) Blum, J.; Amer, I.; Vollhardt, K. P. C.; Schwarz, H.; Hohne, G. J. *Org. Chem.* **1987**, *52*, 2804–2813.
- (15) Weddle, K. S.; Aiken, J. D.; Finke, R. G. *J. Am. Chem. Soc.* **1998**, *120*, 5653–5666.
- (16) Roucoux, A.; Schulz, J.; Patin, H. *Chem. Rev.* **2002**, *102*, 3757–3778.
- (17) Xiong, Y.; Wiley, B. J.; Xia, Y. *Angew. Chem., Int. Ed.* **2007**, *46*, 7157–7159.
- (18) Finney, E. E.; Finke, R. G. *J. Colloid Interface Sci.* **2008**, *317*, 351–374.
- (19) *Nanoparticles and Catalysis*; Astruc, D., Ed.; Wiley-VCH: Weinheim, Germany, 2008.
- (20) Park, J. H.; Chung, Y. K. *Dalton Trans.* **2008**, 2369–2378.
- (21) Yuge, K. *Phys. Rev. B* **2011**, *84*, 085451.
- (22) Yuge, K. *Mater. Trans.* **2011**, *52*, 1339–1343.
- (23) Renzas, J. R.; Huang, W. Y.; Zhang, Y. W.; Grass, M. E.; Somorjai, G. A. *Catal. Lett.* **2011**, *141*, 235–241.
- (24) Essinger-Hileman, E. R.; DeCicco, D.; Bondi, J. F.; Schaak, R. E. *J. Mater. Chem.* **2011**, *21*, 11599–11604.
- (25) Renzas, J. R.; Huang, W. Y.; Zhang, Y. W.; Grass, M. E.; Hoang, D. T.; Alayoglu, S.; Butcher, D. R.; Tao, F.; Liu, Z.; Somorjai, G. A. *Phys. Chem. Chem. Phys.* **2011**, *13*, 2556–2562.
- (26) Pan, H. B.; Wai, C. M. *New J. Chem.* **2011**, *35*, 1649–1660.
- (27) Matsushita, T.; Shiraiishi, Y.; Horiuchi, S.; Toshima, N. *Bull. Chem. Soc. Jpn.* **2007**, *80*, 1217–1225.
- (28) Boutros, M.; Shirley, G.; Onfroy, T.; Launay, F. *Appl. Catal., A* **2011**, *394*, 158–165.
- (29) Sadykov, V. A.; Tikhov, S. F.; Tsybulya, S. V.; Kryukova, G. N.; Veniaminov, S. A.; Kolomiichuk, V. N.; Bulgakov, N. N.; Isupova, L. A.; Paukshtis, E. A.; Zaikovskii, V. I.; Kustova, G. N.; Burgina, L. B. *Stud. Surf. Sci. Catal.* **1997**, *110*, 1155–1164.
- (30) Jacobs, P. W.; Somorjai, G. A. *J. Mol. Catal. A: Chem.* **1998**, *131*, 5–18.
- (31) Singh, U. K.; Vannice, M. A. *Appl. Catal., A* **2001**, *213*, 1–24.
- (32) Norskov, J. K.; Bligaard, T.; Hvolbaek, B.; Abild-Pedersen, F.; Chorkendorff, I.; Christensen, C. H. *Chem. Soc. Rev.* **2008**, *37*, 2163–2171.
- (33) Van, S. R. A. *Acc. Chem. Res.* **2009**, *42*, 57–66.
- (34) McClure, S. M.; Lundwall, M.; Yang, F.; Zhou, Z.; Goodman, D. W. *J. Phys.: Condens. Matter* **2009**, *21*, 474223/1–474223/7.
- (35) Oh, S. H.; Fisher, G. B.; Carpenter, J. E.; Goodman, D. W. *J. Catal.* **1986**, *100*, 360–376.
- (36) Grass, M. E.; Zhang, Y.; Butcher, D. R.; Park, J. Y.; Li, Y.; Bluhm, H.; Bratlie, K. M.; Zhang, T.; Somorjai, G. A. *Angew. Chem., Int. Ed.* **2008**, *47*, 8893–8896.
- (37) Grass, M. E.; Joo, S. H.; Zhang, Y.; Somorjai, G. A. *J. Phys. Chem. C* **2009**, *113*, 8616–8623.
- (38) Lighthart, D. A. J. M.; van, S. R. A.; Hensen, E. J. M. *Angew. Chem., Int. Ed.* **2011**, *50*, 5306–5310, S5306/5301–S5306/5309.
- (39) Lighthart, D. A. J. M.; van, S. R. A.; Hensen, E. J. M. *J. Catal.* **2011**, *280*, 206–220.
- (40) Hindle, K. T.; Jackson, S. D.; Stirling, D.; Webb, G. J. *Catal.* **2006**, *241*, 417–425.
- (41) Pan, H.-B.; Wai, C. M. *J. Phys. Chem. C* **2010**, *114*, 11364–11369.
- (42) Dyson, P. J. *Dalton Trans.* **2003**, 2964–2974.
- (43) Kapur, N.; Hyun, J.; Shan, B.; Nicholas, J. B.; Cho, K. J. *Phys. Chem. C* **2010**, *114*, 10171–10182.
- (44) Bruss, A. J.; Gelesky, M. A.; Machado, G.; Dupont, J. J. *Mol. Catal. A: Chem.* **2006**, *252*, 212–218.
- (45) McClure, S. M.; Lundwall, M. J.; Goodman, D. W. *Proc. Natl. Acad. Sci. U. S. A.* **2011**, *108*, 931–936, S931/931–S931/933.
- (46) Yan, L.; Ding, Y. J.; Lin, L. W.; Zhu, H. J.; Yin, H. M.; Li, X. M.; Lu, Y. *J. Mol. Catal. A: Chem.* **2009**, *300*, 116–120.
- (47) Han, M.; Liu, H. *Macromol. Symp.* **1996**, *105*, 179–183.
- (48) Yates, D. J. C.; Sinfelt, J. H. *J. Catal.* **1967**, *8*, 348–358.
- (49) Sinfelt, J. H.; Yates, D. J. C. *J. Catal.* **1967**, *8*, 82–90.
- (50) Siani, A.; Alexeev, O. S.; Deutsch, D. S.; Monnier, J. R.; Fanson, P. T.; Hirata, H.; Matsumoto, S.; Williams, C. T.; Amiridis, M. D. *J. Catal.* **2009**, *266*, 331–342.
- (51) Chen, B.; Goodwin, J. G. *J. Catal.* **1996**, *158*, 228–235.
- (52) Ojeda, M.; Rojas, S.; Boutonnet, M.; Perez-Alonso, F. J.; Javier, G.-G. F.; Fierro, J. L. G. *Appl. Catal., A* **2004**, *274*, 33–41.
- (53) Hoxha, F.; van Vegten, N.; Urakawa, A.; Krurneich, F.; Mallat, T.; Baiker, A. *J. Catal.* **2009**, *261*, 224–231.
- (54) Kanuru, V. K.; Humphrey, S. M.; Kyffin, J. M. W.; Jefferson, D. A.; Burton, J. W.; Armbruster, M.; Lambert, R. M. *Dalton Trans.* **2009**, 7602–7605.

- (55) Han, D. F.; Li, X. H.; Zhang, H. D.; Liu, Z. M.; Li, J.; Li, C. J. *Catal.* **2006**, *243*, 318–328.
- (56) Xia, Y.; Xiong, Y.; Lim, B.; Skrabalak, S. E. *Angew. Chem., Int. Ed.* **2009**, *48*, 60–103.
- (57) Zhang, Y.; Grass, M. E.; Kuhn, J. N.; Tao, F.; Habas, S. E.; Huang, W.; Yang, P.; Somorjai, G. A. *J. Am. Chem. Soc.* **2008**, *130*, 5868–5869.
- (58) Kundu, S.; Wang, K.; Liang, H. J. *Phys. Chem. C* **2009**, *113*, 18570–18577.
- (59) Zhang, Y.; Grass, M. E.; Huang, W.; Somorjai, G. A. *Langmuir* **2010**, *26*, 16463–16468.
- (60) Park, K. H.; Jang, K.; Kim, H. J.; Son, S. U. *Angew. Chem., Int. Ed.* **2007**, *46*, 1152–1155.
- (61) Nguyen, V.-L.; Nguyen, D.-C.; Hirata, H.; Matsubara, T.; Ohtaki, M.; Nogami, M. *J. Cryst. Growth* **2011**, *320*, 78–89.
- (62) Zetsu, N.; McLellan, J. M.; Wiley, B.; Yin, Y.; Li, Z.-Y.; Xia, Y. *Angew. Chem., Int. Ed.* **2006**, *45*, 1288–1292.
- (63) Biacchi, A. J.; Schaak, R. E. *ACS Nano* **2011**, *5*, 8089–8099.
- (64) Zhou, K.; Li, Y. *Angew. Chem., Int. Ed.* **2012**, *51*, 602–613.
- (65) Renzas, J. R.; Zhang, Y.; Huang, W.; Somorjai, G. A. *Catal. Lett.* **2009**, *132*, 317–322.
- (66) Peden, C. H. F.; Belton, D. N.; Schmieg, S. J. *J. Catal.* **1995**, *155*, 204–218.
- (67) Yuan, Q.; Zhou, Z.; Zhuang, J.; Wang, X. *Inorg. Chem.* **2010**, *49*, 5515–5521.
- (68) Nolte, P.; Stierle, A.; Jin-Phillipp, N. Y.; Kasper, N.; Schulli, T. U.; Dosch, H. *Science* **2008**, *321*, 1654–1658.
- (69) Corma, A.; Garcia, H. *Chem. Rev.* **2002**, *102*, 3837–3892.
- (70) Hubert, C.; Denicourt-Nowicki, A.; Guegan, J. P.; Roucoux, A. *Dalton Trans.* **2009**, 7356–7358.
- (71) Guyonnet, B. E.; Sassine, R.; Denicourt-Nowicki, A.; Launay, F.; Roucoux, A. *Dalton Trans.* **2011**, *40*, 6524–6531.
- (72) Lu, Y. D.; Wang, Y. H.; Jin, Z. L. *Chin. Chem. Lett.* **2010**, *21*, 1067–1070.
- (73) Snelders, D. J. M.; Yan, N.; Gan, W.; Laurency, G.; Dyson, P. J. *ACS Catal.* **2012**, *2*, 201–207.
- (74) Mevellec, V.; Leger, B.; Mauduit, M.; Roucoux, A. *Chem. Commun.* **2005**, 2838–2839.
- (75) Mu, X. D.; Meng, J. Q.; Li, Z. C.; Kou, Y. *J. Am. Chem. Soc.* **2005**, *127*, 9694–9695.
- (76) Gelesky, M. A.; Chiaro, S. S. X.; Pavan, F. A.; dos Santos, J. H. Z.; Dupont, J. *Dalton Trans.* **2007**, 5549–5553.
- (77) Zhao, C.; Wang, H.-Z.; Yan, N.; Xiao, C.-X.; Mu, X.-D.; Dyson, P. J.; Kou, Y. *J. Catal.* **2007**, *250*, 33–40.
- (78) Leger, B.; Denicourt-Nowicki, A.; Olivier-Bourbigou, H.; Roucoux, A. *ChemSusChem* **2008**, *1*, 984–987.
- (79) Leger, B.; Denicourt-Nowicki, A.; Olivier-Bourbigou, H.; Roucoux, A. *Inorg. Chem.* **2008**, *47*, 9090–9096.
- (80) Leger, B.; Denicourt-Nowicki, A.; Olivier-Bourbigou, H.; Roucoux, A. *Tetrahedron Lett.* **2009**, *50*, 6531–6533.
- (81) Yang, X.; Yan, N.; Fei, Z.; Crespo-Quesada, R. M.; Laurency, G.; Kiwi-Minsker, L.; Kou, Y.; Li, Y.; Dyson, P. J. *Inorg. Chem.* **2008**, *47*, 7444–7446.
- (82) Vollmer, C.; Redel, E.; Abu-Shandi, K.; Thomann, R.; Manyar, H.; Hardacre, C.; Janiak, C. *Chem.—Eur. J.* **2010**, *16*, 3849–3858.
- (83) Yan, N.; Yuan, Y.; Dykeman, R.; Kou, Y.; Dyson, P. J. *Angew. Chem., Int. Ed.* **2010**, *49*, 5549–5553.
- (84) Dykeman, R. R.; Yan, N.; Scopelliti, R.; Dyson, P. J. *Inorg. Chem.* **2011**, *50*, 717–719.
- (85) Yan, N.; Yuan, Y.; Dyson, P. J. *Chem. Commun.* **2011**, *47*, 2529–2531.
- (86) Cimpeanu, V.; Kocivar, M.; Parvulescu, V. I.; Leitner, W. *Angew. Chem., Int. Ed.* **2009**, *48*, 1085–1088.
- (87) Jutz, F.; Andanson, J.-M.; Baiker, A. *J. Catal.* **2009**, *268*, 356–366.
- (88) Quek, X. Y.; Guan, Y. J.; van Santen, R. A.; Hensen, E. J. M. *ChemSusChem* **2010**, *3*, 1264–1267.
- (89) Stratton, S. A.; Luska, K. L.; Moores, A. *Catal. Today* **2012**, DOI: 10.1016/j.cattod.2011.1009.1016.
- (90) Nakamura, I.; Yamanoi, Y.; Yonezawa, T.; Imaoka, T.; Yamamoto, K.; Nishihara, H. *Chem. Commun.* **2008**, 5716–5718.
- (91) Yan, N.; Zhang, J.-g.; Tong, Y.; Yao, S.; Xiao, C.; Li, Z.; Kou, Y. *Chem. Commun.* **2009**, 4423–4425.
- (92) Chen, Z. J.; Wang, Y. H.; Jiang, J. Y.; Jin, Z. L. *Chin. J. Catal.* **2011**, *32*, 1133–1137.
- (93) Zahmakiran, M.; Ozkar, S. *Inorg. Chem.* **2009**, *48*, 8955–8964.
- (94) Leger, B.; Denicourt-Nowicki, A.; Roucoux, A.; Olivier-Bourbigou, H. *Adv. Synth. Catal.* **2008**, *350*, 153–159.
- (95) Denicourt-Nowicki, A.; Leger, B.; Roucoux, A. *Phys. Chem. Chem. Phys.* **2011**, *13*, 13510–13517.
- (96) Fonseca, G. S.; Scholten, J. D.; Dupont, J. *Synlett* **2004**, 1525–1528.
- (97) Pittelkow, M.; Brock-Nannestad, T.; Moth-Poulsen, K.; Christensen, J. B. *Chem. Commun.* **2008**, 2358–2360.
- (98) Studer, M.; Blaser, H. U.; Exner, C. *Adv. Synth. Catal.* **2003**, *345*, 45–65.
- (99) Berthod, M.; Mignani, G.; Woodward, G.; Lemaire, M. *Chem. Rev.* **2005**, *105*, 1801–1836.
- (100) Axet, M. R.; Castillon, S.; Claver, C.; Philippot, K.; Lecante, P.; Chaudret, B. *Eur. J. Inorg. Chem.* **2008**, 3460–3466.
- (101) Gual, A.; Godard, C.; Philippot, K.; Chaudret, B.; Denicourt-Nowicki, A.; Roucoux, A.; Castillon, S.; Claver, C. *ChemSusChem* **2009**, *2*, 769–779.
- (102) Favier, I.; Gomez, M.; Muller, G.; Picurelli, D.; Nowicki, A.; Roucoux, A.; Bou, J. *J. Appl. Polym. Sci.* **2007**, *105*, 2772–2782.
- (103) Guyonnet, B. E.; Denicourt-Nowicki, A.; Sassine, R.; Beaunier, P.; Launay, F.; Roucoux, A. *ChemSusChem* **2010**, *3*, 1276–1279.
- (104) Han, D.; Li, X.; Zhang, H.; Liu, Z.; Hu, G.; Li, C. *J. Mol. Catal. A: Chem.* **2008**, *283*, 15–22.
- (105) Jaska, C. A.; Manners, I. *J. Am. Chem. Soc.* **2004**, *126*, 2698–2699.
- (106) Hubert, C.; Bile, E. G.; Denicourt-Nowicki, A.; Roucoux, A. *Green Chem.* **2011**, *13*, 1766–1771.
- (107) Hubert, C.; Bile, E. G.; Denicourt-Nowicki, A.; Roucoux, A. *Appl. Catal., A* **2011**, *394*, 215–219.
- (108) Yan, N.; Xiao, C.; Kou, Y. *Coord. Chem. Rev.* **2010**, *254*, 1179–1218.
- (109) Corma, A.; Garcia, H. *Chem. Rev.* **2003**, *103*, 4307–4365.
- (110) Choi, S. M.; Seo, M. H.; Kim, H.; Kim, W. B. *Synth. Met.* **2011**, *161*, 2405–2411.
- (111) Marquardt, D.; Vollmer, C.; Thomann, R.; Steurer, P.; Muelhaupt, R.; Redel, E.; Janiak, C. *Carbon* **2011**, *49*, 1326–1332.
- (112) Yoon, B.; Wai, C. M. *J. Am. Chem. Soc.* **2005**, *127*, 17174–17175.
- (113) Kakade, B. A.; Sahoo, S.; Halligudi, S. B.; Pillai, V. K. *J. Phys. Chem. C* **2008**, *112*, 13317–13319.
- (114) Pan, H.-B.; Wai, C. M. *J. Phys. Chem. C* **2009**, *113*, 19782–19788.
- (115) Liu, H.-W.; Pan, H.-B.; Tian, G.-X.; Chen, H.-J.; Chiu, K.-H.; Jen, J.-F.; Lo, J.-G.; Wai, C. M. *Synth. Commun.* **2011**, *41*, 2624–2630.
- (116) Wang, H.; Zhao, F.; Fujita, S.-I.; Arai, M. *Catal. Commun.* **2008**, *9*, 362–368.
- (117) Motoyama, Y.; Takasaki, M.; Yoon, S.-H.; Mochida, I.; Nagashima, H. *Org. Lett.* **2009**, *11*, 5042–5045.
- (118) Harada, T.; Ikeda, S.; Ng, Y. H.; Sakata, T.; Mori, H.; Torimoto, T.; Matsumura, M. *Adv. Funct. Mater.* **2008**, *18*, 2190–2196.
- (119) Luo, P. F.; Xu, K. L.; Zhang, R.; Huang, L.; Wang, J.; Xing, W. H.; Huang, J. *Catal. Sci. Technol.* **2012**, *2*, 301–304.
- (120) Zahmakiran, M.; Román-Leshkov, Y.; Zhang, Y. *Langmuir* **2011**, *28*, 60–64.
- (121) Boutros, M.; Denicourt-Nowicki, A.; Roucoux, A.; Gengembre, L.; Beaunier, P.; Gedeon, A.; Launay, F. *Chem. Commun.* **2008**, 2920–2922.
- (122) Park, I. S.; Kwon, M. S.; Kang, K. Y.; Lee, J. S.; Park, J. *Adv. Synth. Catal.* **2007**, *349*, 2039–2047.
- (123) Gelesky, M. A.; Scheeren, C. W.; Foppa, L.; Pavan, F. A.; Dias, S. L. P.; Dupont, J. *Biomacromolecules* **2009**, *10*, 1888–1893.

- (124) Chen, W.-M.; Ding, Y.-J.; Jiang, D.-H.; Wang, T.; Luo, H.-Y. *Catal. Commun.* **2006**, *7*, 559–562.
- (125) Huang, W.; Kuhn, J. N.; Tsung, C. K.; Zhang, Y.; Habas, S. E.; Yang, P.; Somorjai, G. A. *Nano Lett.* **2008**, *8*, 2027–2034.
- (126) Barthe, L.; Hemati, M.; Philippot, K.; Chaudret, B.; Denicourt-Nowicki, A.; Roucoux, A. *Chem. Eng. J.* **2009**, *151*, 372–379.
- (127) Hubert, C.; Denicourt-Nowicki, A.; Beaunier, P.; Roucoux, A. *Green Chem.* **2010**, *12*, 1167–1170.
- (128) Eilbracht, P.; Barfacker, L.; Buss, C.; Hollmann, C.; Kitsos-Rzychon, B. E.; Kranemann, C. L.; Rische, T.; Roggenbuck, R.; Schmidt, A. *Chem. Rev.* **1999**, *99*, 3329–3365.
- (129) Haumann, M.; Riisager, A. *Chem. Rev.* **2008**, *108*, 1474–1497.
- (130) Bergbreiter, D. E.; Tian, J. H.; Hongfa, C. *Chem. Rev.* **2009**, *109*, 530–582.
- (131) Hebrard, F.; Kalck, P. *Chem. Rev.* **2009**, *109*, 4272–4282.
- (132) Redel, E.; Kramer, J.; Thomann, R.; Janiak, C. *J. Organomet. Chem.* **2009**, *694*, 1069–1075.
- (133) Scholten, J. D.; Leal, B. C.; Dupont, J. *ACS Catal.* **2012**, *2*, 184–200.
- (134) Luska, K. L.; Moores, A. *ChemCatChem* **2011**, DOI: 10.1002/cctc.201100366.
- (135) Dahl, J. A.; Maddux, B. L. S.; Hutchison, J. E. *Chem. Rev.* **2007**, *107*, 2228–2269.
- (136) Parvulescu, V. I.; Hardacre, C. *Chem. Rev.* **2007**, *107*, 2615–2665.
- (137) Hallett, J. P.; Welton, T. *Chem. Rev.* **2011**, *111*, 3508–3576.
- (138) Jacinto, M. J.; Kiyohara, P. K.; Masunaga, S. H.; Jardim, R. F.; Rossi, L. M. *Appl. Catal., A* **2008**, *338*, 52–57.
- (139) Yan, N.; Zhang, J.; Yuan, Y.; Chen, G.-T.; Dyson, P. J.; Li, Z.-C.; Kou, Y. *Chem. Commun.* **2010**, *46*, 1631–1633.
- (140) Yuan, Y.; Yan, N.; Dyson, P. J. *Inorg. Chem.* **2011**, *50*, 11069–11074.
- (141) Dimick, P. S.; Herman, R. G.; Lyman, C. E. *Catal. Lett.* **2010**, *135*, 33–40.